Weather and Climate Extremes 34 (2021) 100387

Contents lists available at ScienceDirect

Weather and Climate Extremes

journal homepage: www.elsevier.com/locate/wace

Modulation of mid-Atlantic tropical cyclone landfalls by the Madden-Julian Oscillation

Julia V. Manganello *, James L. Kinter III

Center for Ocean-Land-Atmosphere Studies (COLA), George Mason University, Fairfax, VA, USA

ARTICLE INFO

Keywords:
A high-atmospheric-resolution seasonal prediction system is used to investigate the link between mid-Atlantic TC landfalls and the MJO
Between 14- and 7-day lead times, TC landfalls are more likely to occur during MJO phases 1 and 7, which is supported by observational data
In the short range (between 6-day lead and landfall), MJO phase 1 is strongly favored with some contribution from phases 2 and 3

ABSTRACT

Tropical cyclone (TC) landfalls over the U.S. mid-Atlantic region are very infrequent. However, when they do occur, the resulting human and material losses can be severe, as was the case with Hurricane Sandy in 2012. Therefore, it is important to predict these land-falling events as far in advance as possible. In this study, we investigate the relationship between mid-Atlantic TC landfalls and the Madden-Julian Oscillation (MJO), which is the dominant source of climate variability in the tropics on intraseasonal time scales. This is largely accomplished by using a high-atmospheric-resolution ensemble prediction system based on the European Centre for Medium-Range Weather Forecasts (ECMWF) operational model (Project Minerva) to compile the statistics of these rare events, and the velocity potential MJO (VPM) index to define the phase and amplitude of the MJO. We find that at longer lead times (between 14 and 7 days prior to landfall), statistically significant peak landfall probabilities are present during MJO phases 1 and 7 and, to some extent, phase 8. This result is largely supported by observational data. At shorter lead times (between 6-day lead and landfall), phase 1 is strongly favored with some contribution from phases 2 and 3. These findings suggest a potential for extended-range predictions of the mid-Atlantic TC landfall risk based on the phase of the MJO.

1. Introduction

Tropical cyclones (TCs) are among the most hazardous extreme weather events that can lead to large human and material losses when they come in close proximity to land. Although considered as one of the most infrequent landfalls along the U.S. East Coast, TC landfalls over the mid-Atlantic,[1] when they do occur, can have devastating consequences due to large concentration of population and wealth in the region. A recent example is Hurricane Sandy in 2012 (Blake et al., 2013; NHC, 2018).

TC landfall is a complex phenomenon whose probability depends on the following fundamental factors: 1) genesis, 2) development (the intensity life cycle), and 3) the shape of track (the storm's ability to approach the coastline; Dailey et al., 2009). The Madden-Julian Oscillation (MJO), which is the leading intraseasonal mode of atmospheric and oceanic variability in the tropics (see Li (2014) for a review), is found to influence some of these aspects of the North Atlantic TC activity. The MJO is a global-scale oscillation in circulation coupled to large-scale variations in convection. Its characteristic feature is the eastward propagation from the Indian Ocean into the central Pacific where the upper tropospheric anomalies of zonal wind and the velocity potential are observed to circle the globe in about 50 days (Madden and Julian, 1994). This periodicity represents a major source of predictability on subseasonal time scales. Associated with the MJO variability are large-scale variations in upper- and lower-level winds, temperature, sea level pressure, convection, atmospheric moisture content, and sea surface temperature. Through these changes and related variations in vertical wind shear (VWS), low-level vorticity and the African easterly wave (AEW) activity, the MJO has been found to modulate TC genesis and development in the North Atlantic (Mo, 2000; Barrett and Leslie, 2009; Vitart, 2009; Klotzbach, 2010; Ventrice et al., 2011; Klotzbach and Oliver, 2015), the overall North Atlantic TC landfall activity (Barrett and Leslie, 2009; Vitart, 2009) and the U.S. TC landfall frequency (Klotzbatch, 2010). The increase of TC activity has been found to occur during the phases of the MJO corresponding to the enhanced convection over parts of Africa and the Indian Ocean and suppressed convection over the tropical Pacific. However, any effects of the MJO on the likelihood of storm recurvature by means of, e.g., changes in the mid-latitude flow patterns, have not been identified in the studies above.

Recent studies with the state-of-the-art sub-seasonal ensemble

* Corresponding author.
E-mail addresses: jvisneva@gmu.edu (J.V. Manganello), ikinter@gmu.edu (J.L. Kinter).

https://doi.org/10.1016/j.wace.2021.100387
Received 17 March 2021; Received in revised form 17 September 2021; Accepted 5 October 2021
Available online 7 October 2021

Table 1
Names and landfall dates of all mid-Atlantic TC landfalls that took place during 1905–2015 according to criteria and definitions detailed in Manganello et al. (2019). Obtained from IBTrACS, version v03r07.

Name of the tropical cyclone	Landfall date
Hurricane #6	08/23/1933
Tropical Storm #7	09/30/1943
Hurricane Connie	08/13/1955
Tropical Storm #6	09/14/1961
Hurricane Doria	09/17/1967
Tropical Storm Doria	08/28/1971
Tropical Storm Dean	09/30/1983
Hurricane Bertha	07/13/1996
Hurricane Floyd	09/16/1999
Hurricane Irene	08/28/2011
Hurricane Sandy	10/29/2012

prediction systems have been able to demonstrate skillful forecasts of the North Atlantic TC genesis at one- to five-week lead times depending on the model (e.g., Jiang et al., 2018; Lee et al., 2018). Probabilistic forecasts of TC occurrence (genesis and subsequent locations) and accumulated cyclone energy (ACE; Bell et al., 2000) have shown skill up to four weeks in advance (Lee et al., 2020). The models' skill scores were found to be dependent on the accurate representation of the TC climatology, the MJO and the MJO-TC relationship. TCs with higher genesis skill were also associated with the convectively active region of the MJO and enhanced low-level vorticity of synoptic-scale waves.

The role of the MJO in the genesis, life cycle and track of Hurricane Sandy has also been investigated. Shen et al. (2013) and Xiang et al. (2015) have both found the genesis of Hurricane Sandy to be highly predictable with a maximum prediction lead time of up to 6 and 11 days, respectively. This relatively high predictability of storm formation, initial development and trajectory was partly attributed to the role of the MJO and its skillful prediction. Xiang et al. (2015) have also predicted Sandy's landfall location and time with one-week lead time (after the genesis has occurred). The authors hypothesized that the predictability source for the landfall of Sandy may also be linked to the MJO. A recent study of Ding et al. (2019) has specifically addressed predictability of Sandy's steering flow. They found that this flow was primarily controlled by a pair of anticyclonic and cyclonic intraseasonal-scale circulation systems. The anticyclone to the north was part of a global wave train triggered by the MJO heating in the tropical Indian Ocean. Accurate simulation of this meridional dipole structure was shown to be a key for a successful extended-range prediction of Sandy's track.

Using a high-atmospheric-resolution coupled prediction system, Manganello et al. (2019) have assessed predictability of all mid-Atlantic TC landfalls that, in addition to the so-called Sandy-like, or westward-curving, tracks also include the late recurving systems like Hurricanes Bertha (1996) and Floyd (1999). Results of this study echo some of the findings of Ding et al. (2019). For example, mean atmospheric circulation anomalies during these land-falling events were found to be similar to the large–scale flow patterns that occurred during Hurricane Sandy. Their analysis using local finite-amplitude wave activity diagnostic (LWA; Huang and Nakamura, 2016) revealed large-amplitude quasi-stationary features extending from the North Atlantic to the North Pacific that persist up to about a week leading to these TC landfalls. In addition, the concurrent atmospheric flow changes over the tropical Atlantic, which were found to be favorable for TC formation and development, were accompanied by coherent anomalies in the tropical Indian Ocean indicative of the enhanced convection in the region.

Motivated by the studies above, we extend the analysis of Manganello et al. (2019) here to investigate a potential link between mid-Atlantic TC landfalls and the MJO. For this purpose, we use (1) ensemble seasonal hindcasts to simulate these rare land-falling events and (2) the velocity potential MJO (VPM) index of Ventrice et al. (2013) as an MJO phase and amplitude diagnostic. It is demonstrated that the MJO significantly modulates mid-Atlantic TC landfalls in this set of simulations suggesting a possibility of extended-range[2] dynamical TC landfall risk predictions in the region beyond the short-range predictions as shown in Manganello et al. (2019). We would like to emphasize that predictability of the observed TC landfalls is not evaluated in this study. Rather, the initialized seasonal forecast data is used as a surrogate for observations due to the limited number of observed landfalls. This is further elaborated in section 2, which briefly introduces model and observational data and numerical methods. Results are presented in section 3. Discussion and some concluding remarks are provided in section 4.

2. Data and methodology

2.1. Numerical experiments

Due to the very few occurrences of mid-Atlantic TC landfalls in the observational record (see section 2.3 below), we largely rely in this analysis on ensemble seasonal hindcasts performed with the Minerva forecasting system to compile the statistics of these rare events. Minerva is an experimental coupled prediction system (EPS) based on the European Centre for Medium-Range Weather Forecasts (ECMWF) System 4 (see Manganello et al. (2016) for full details). The Nucleus for European Modeling of the Ocean (NEMO; Madec, 2008) version 3.0 is the ocean component model of this EPS. NEMO has the ORCA1 grid with a horizontal resolution of about 1° (and the equatorial refinement of 1/3°) and 42 levels in the vertical. The atmospheric component model is the ECMWF Integrated Forecasting System (IFS; European Centre for Medium-Range Weather Forecasts, 2013), cycle 38r1, which is a spectral, semi-implicit, semi-Lagrangian hydrostatic model with 91 levels in the vertical, and a model top in the mesosphere at 0.01 hPa. The unperturbed initial conditions for the atmosphere come from the ECMWF interim reanalysis (ERA-I; Dee et al., 2011) and Ocean ReAnalysis System 4 (ORA-S4; Balmaseda et al., 2013) for the ocean.

In this study, we use experiments in which the horizontal resolution of the IFS is spectral triangular truncation with 1279 wave numbers (referred to as T1279 hereafter), corresponding approximately to 16-km grid spacing. Minerva retrospective forecasts are initialized on May 1 during 1980–2013, are of 7-month duration and consist of 15 ensemble members, which effectively represents 510 May–November seasons. The data is aggregated together (rather than separated by forecast lead time) to increase statistical significance. The focus of this study is exclusively on the July–October (JASO) season as the peak season of mid-Atlantic TC landfall activity (see Fig. 4a in Manganello et al., 2019). Forecasts initialized on July 1 would have been preferred for this purpose but were not available from the Minerva data set. Simulated upper-air data used in this analysis is truncated at spectral T42 resolution.

2.2. Identification and tracking of tropical cyclones

Simulated TCs are identified explicitly in the model data based on the tracking algorithm of Hodges (1994, 1995, 1999). Vortices are detected as maxima in the 6-hourly relative vorticity field averaged between 850- and 600-hPa levels with a threshold value of 5×10^{-6} s^{-1} (at a spectral resolution of T63). To separate TCs from the raw tracks, a post-tracking lifetime filter of 2 days and a set of TC identification criteria are applied. The latter include an 1) intensity (10-m wind speed) threshold equivalent to the observed tropical storm intensity, 2) warm core condition, 3) coherent vertical structure condition, 4) duration requirement where the criteria 1–3 need to be jointly attained for at least 24 h at some point

[2] We adopt here the definition of extended-range forecasts by the U.S. National Weather Service corresponding to the forecasts over the next 6–10 and 8–14 days (Xiang et al., 2015).

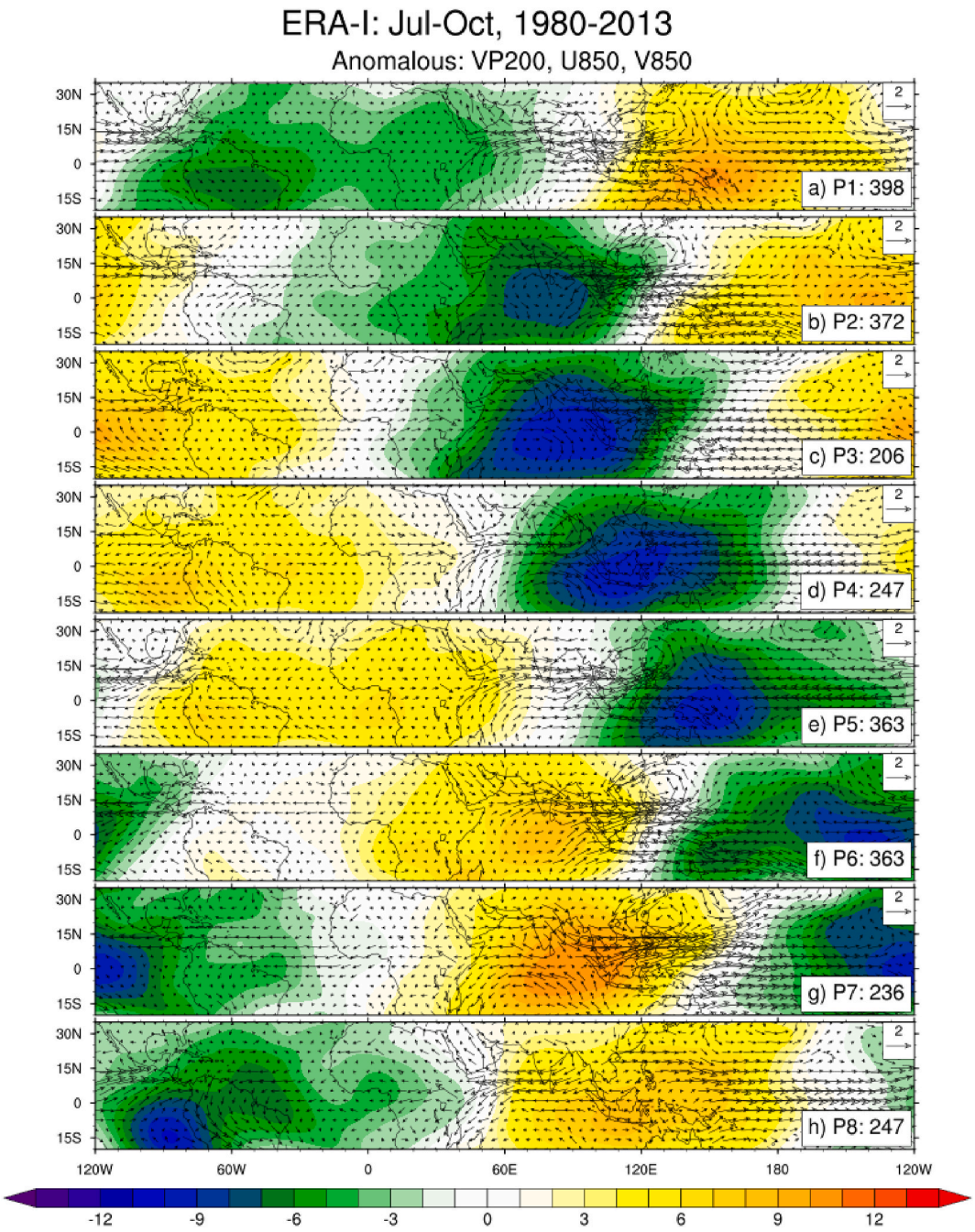

Fig. 1. ERA-I JASO (1980–2013) composites of anomalous 200-hPa velocity potential (shaded) and 850-hPa wind anomalies (vectors) for each MJO phase (indicated in the caption of each panel after letter "P") using the VPM index. Composites are made by averaging over the set of all days for a particular phase when amplitudes of the index are greater or equal to one standard deviation. Total number of days is listed in the caption of each panel. Negative VP200 anomalies represent upper-level divergence. Units are 10^6 m^2s.[11] The reference vector is 2 ms^{-1}.

during the life cycle of a storm, and 5) geographic extent of the first identification (0°-20°N over land and 0°-30°N over oceans).

A mid-Atlantic TC landfall is considered to take place when: 1) the mid-Atlantic coastline is intersected from the sea by a TC track; or 2) the water-to-land transition occurring along the Chesapeake Bay or Delmarva coastlines is preceded by landfall in North Carolina. Although we do not consider only primary landfalls, if a TC makes landfall as described above more than once only the first occurrence is counted. Further details on TC identification and landfall definition in the mid-Atlantic are provided in Manganello et al. (2019).

2.3. Observational data

To validate model results of the MJO phase impact on TC landfall activity we use International Best Track Archive for Climate Stewardship dataset (IBTrACS, Knapp et al., 2010). It contains observed TC track data including post-season analysis of TC positions and maximum sustained wind estimates for all North Atlantic storms from 1851 to present. Consistent with definitions above (section 2.2), only twenty land-falling events in the mid-Atlantic were identified during 1851–2016, and only five during the recent observational period of 1980–2016 (see Manganello et al., 2019). To minimize the uncertainty, we use the longest available observational estimate of the MJO, which is a statistical

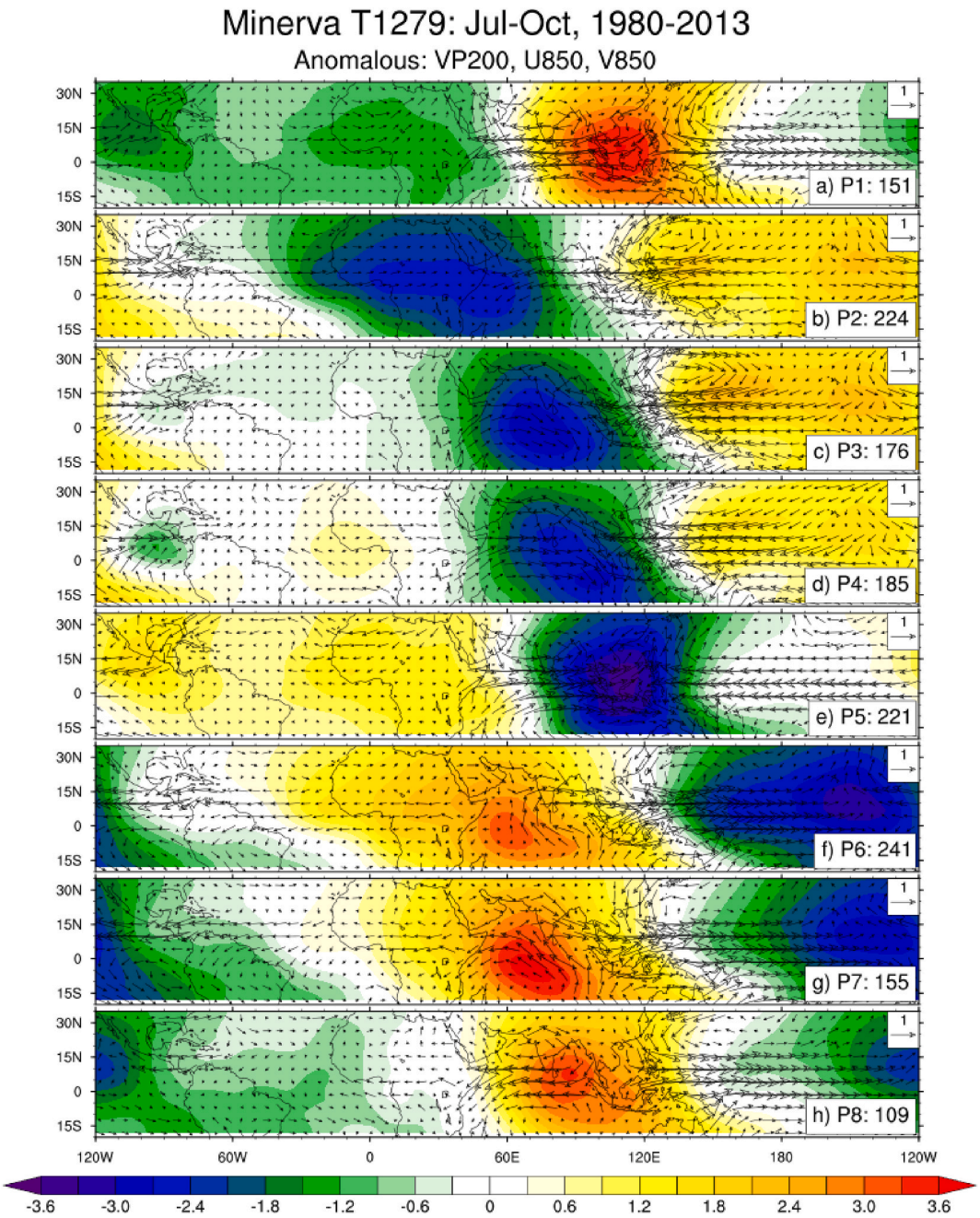

Fig. 2. The same as in Fig. 1 but for the ensemble-mean T1279 hindcast data. Please note the different VP200 scale in this figure compared to Fig. 1. The reference vector is 1 m/s.

reconstruction of the Real-time Multivariate MJO (RMM) index of Wheeler and Hendon (2004) from 1905 to 2015 based on tropical surface pressure from the twentieth-century reanalysis project by Oliver and Thompson (2012). We use the 20CR V3 version of the index downloaded from http://passage.phys.ocean.dal.ca/~olivere/data/mjoindex_IHR_20CRV3.dat. During this time period of 1905–2015, eleven mid-Atlantic TC landfalls took place (see Table 1).

For the observational estimates of upper-air fields, we use the ERA-I at 0.703° x ~0.702° horizontal resolution for the same time period of 1980–2013 as hindcast data. The ERA-I data were downloaded form the Research Data Archive at the National Center for Atmospheric Research, Computational and Information Systems Laboratory (https://doi.org/10.5065/D6CR5RD9, accessed 24 July 2019).

2.4. MJO diagnosis

The daily state (phase and magnitude) of the MJO is determined using the velocity potential MJO (VPM) index of Ventrice et al. (2013). It consists of the leading pair of principal components (PCs) from a combined empirical orthogonal function (EOF) analysis of meridionally averaged (15°N-15°S) 200-hPa zonal wind (U200), 850-hPa zonal wind (U850) and 200-hPa velocity potential (VP200). This index is therefore similar in construction to the RMM index of Wheeler and Hendon except it uses VP200 instead of the outgoing longwave radiation. This change results in better discrimination of the MJO signal during boreal summer using the VPM index compared to the RMM index, including somewhat

[1] Specified here as the coastlines of Virginia, Chesapeake Bay, Delmarva Peninsula, and New Jersey.

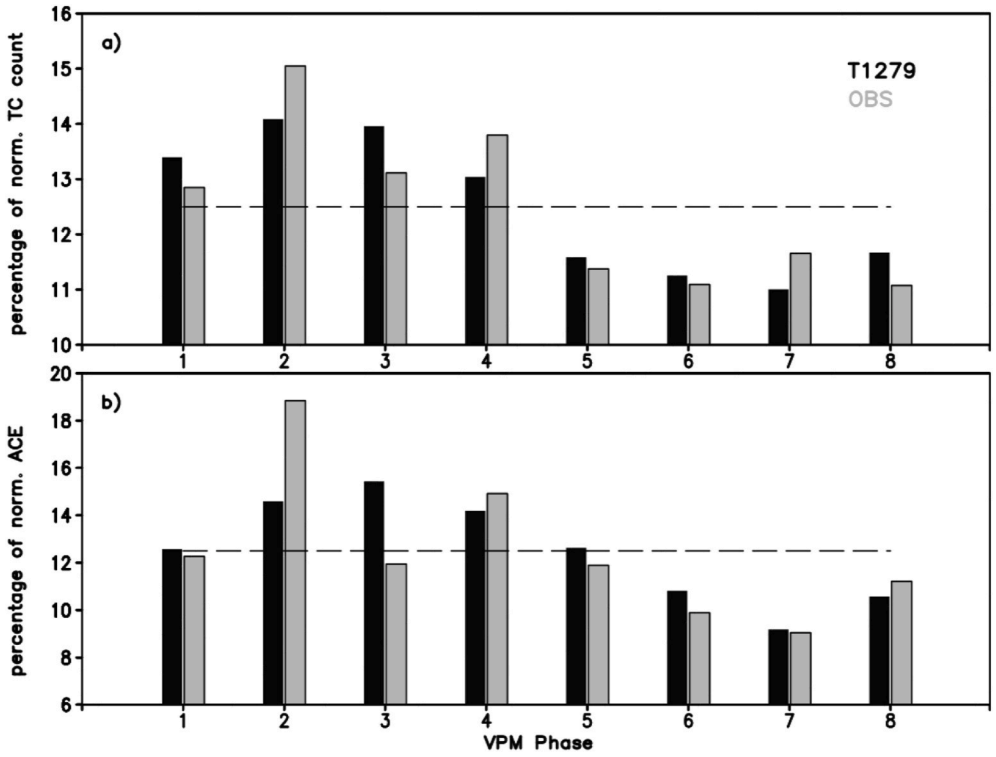

Fig. 3. Observed (grey columns) and simulated (black columns) percentage values of normalized basin-wide TC counts and ACE in each phase of the MJO during strong MJO events (with amplitudes greater or equal to one standard deviation) for the JASO season of 1980–2013. Dashed lines denote the value of 12.5%, which would be the expected activity level during each phase if MJO did not have any effect on the displayed statistics.

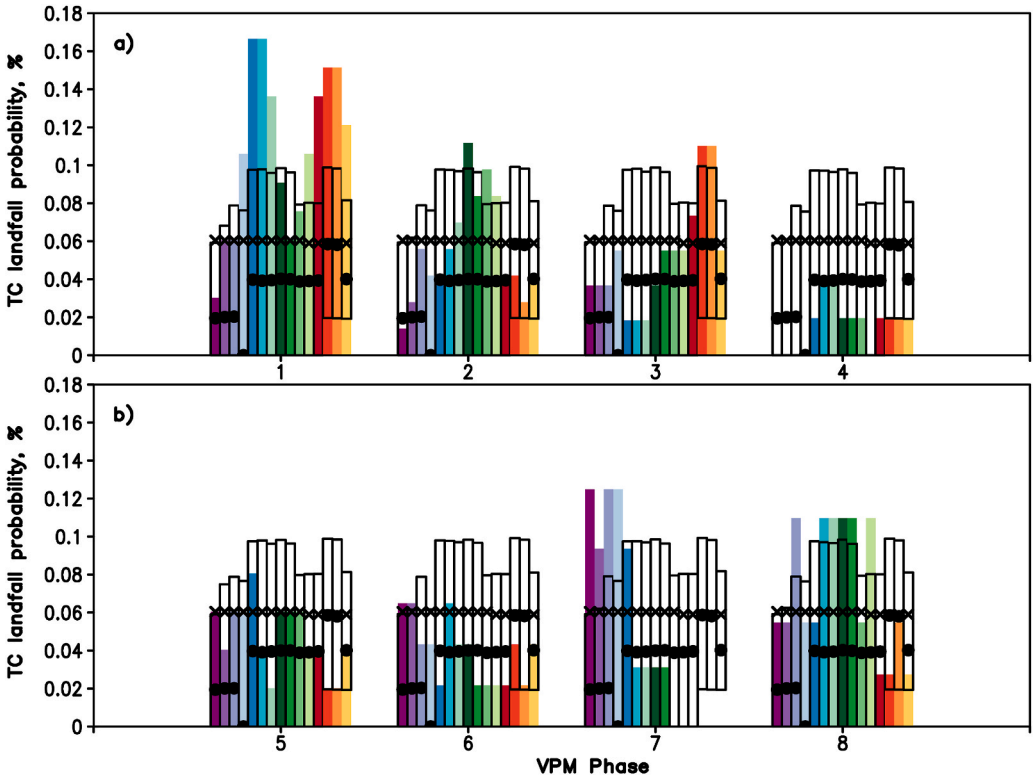

Fig. 4. Probability of mid-Atlantic TC landfalls (%; color bars) in Minerva hindcasts at T1279 for each MJO phase represented by model VPM PCs at different lead times ranging from 14 days (purple bar) to landfall (yellow bar) for the JASO season of 1980–2013. Crosses denote climatological probabilities. Black outlined bars encompass the probabilities between the 10th and 90th percentiles; dots represent the median. See text for more detail. (For interpretation of the references to color in this figure legend, the reader is referred to the Web version of this article.)

stronger and more coherent modulation of Atlantic TC activity (Ventrice et al., 2013).

The VPM index is applied to ERA-I data following the methodology outlined in Ventrice et al. (2013) except that the data are additionally downgraded to T42 for the direct comparison and use with hindcasts (see Text S1 in the Supplemental Information for details). To diagnose

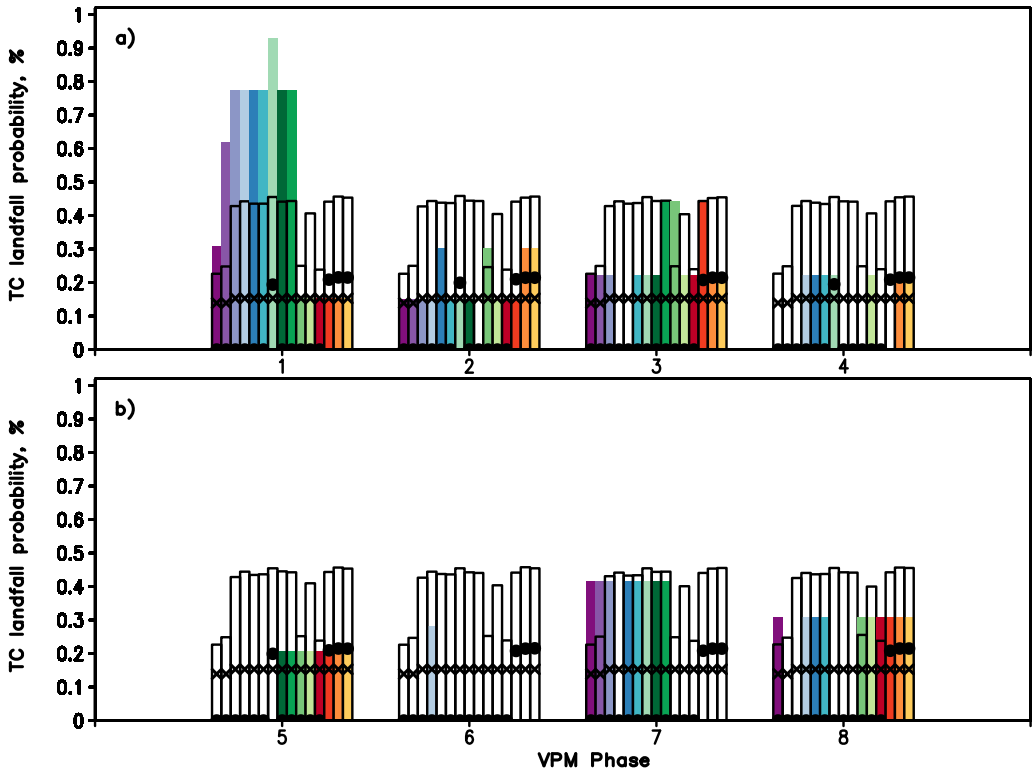

Fig. 5. The same as in Fig. 4, except for the IBTrACS TC data and historical reconstruction of the MJO RMM Index by Oliver and Thompson (2012). Results are based on the JASO season of 1905–2015.

the MJO in the simulations, the hindcast input fields are initially processed following in part the methodology described in Gottschalck et al. (2010) and Vitart (2017). The obtained ERA-I eigenvectors (spatial structures of the leading two EOFs computed from the ERA-I data) form the basis of the VPM index calculation for every ensemble member of the hindcasts and the ensemble mean. This is done by projecting simulated daily anomalies on these ERA-I eigenvectors and normalizing the resultant time series to produce the two-component VPM index (a detailed description of this procedure is provided in Text S2 of the Supplemental Information).

3. Results

Similar to the RMM index, the phase information of the VPM index allows classification of the MJO into eight phases corresponding to a time when it is located over a specific geographical region. The observed composite evolution of the MJO during the boreal summer season using the VPM index is well documented and shown for the JASO season (the peak season of mid-Atlantic TC landfall activity) in Fig. 1. The MJO starts with enhanced convection over the Indian Ocean where it increases in geographical extent and amplitude and moves northward and eastward (phases 1–3). It then propagates across the Maritime continent and into the Pacific (phases 4–6) where a simultaneous northward and eastward propagation is particularly evident in phase 4. The MJO then continues its transit across the Western Hemisphere during phases 7–8. In the Atlantic sector, there are indications of enhanced upper-atmospheric divergence/convection during phases 7, 8, 1 and 2 and anomalous lower-tropospheric westerlies over the tropical North Atlantic during phases 2 and 3. Convective signal over tropical Africa is observed during phases 8, 1–3 including near-equatorial westerly anomalies over the western part of the continent during phases 2 and 3.

Minerva T1279 hindcasts broadly capture the overall phasing and eastward propagation of the MJO, where several deficiencies are also noted (see Fig. 2). Apart from generally weaker magnitudes, upper-level divergence exhibits slower propagation across the Maritime Continent during phases 4 and 5, and no apparent indication of the northward and eastward propagation split compared to observations. Phase speed errors during phases 1–3 are fairly small. Although the eastward propagation in the Pacific is also quite realistic during phases 6–8, there is a relative reduction in the amplitude of the MJO over the tropical Atlantic during phases 7 and 8. These amplitude and phase speed errors are common among ensemble forecasting systems with the ECMWF model generally displaying smaller errors (Vitart, 2017). In addition, convection over Africa is mostly limited to phases 1–3, and near-equatorial westerly anomalies over the western part of the continent are present during phases 1 and 2. Although atmospheric circulation anomalies over the tropical North Atlantic have overall realistic phasing, anomalous low-level westerlies in the region during phase 3 are rather weak.

In addition to the assessment of the quality of MJO forecasts in Minerva, of more direct relevance to this study is the realism of MJO modulation of the simulated TC activity in the North Atlantic. For this purpose, we compute normalized basin-wide TC counts and ACE. These quantities are calculated by dividing the sums of all daily TC counts and total ACE in each MJO VPM phase when the MJO amplitude is greater or equal to one by the number of days that the MJO is in that phase. Fig. 3 shows the percentage of normalized TC counts and ACE in all eight MJO VPM phases (Fig. 3a and b, respectively) for Minerva hindcasts and observations during the JASO season of 1980–2013. We see roughly similar modulation patterns in the observations and hindcasts where TC activity is generally enhanced in VPM phases 1–4 and suppressed during phases 5–8. TC activity during phase 2, though, is systematically higher in the observational data compared to hindcasts. The opposite is true for phase 3. Qualitatively similar modulation patterns are also characteristic of the actual, not the percentage, normalized TC counts and ACE (see Fig. S2 in the Supplemental Information). While the observed ACE is much higher than the simulated, which is rather common, the observed TC counts are substantially lower than the predicted (Fig. S2). We believe that the latter difference stems from our tracking procedure that

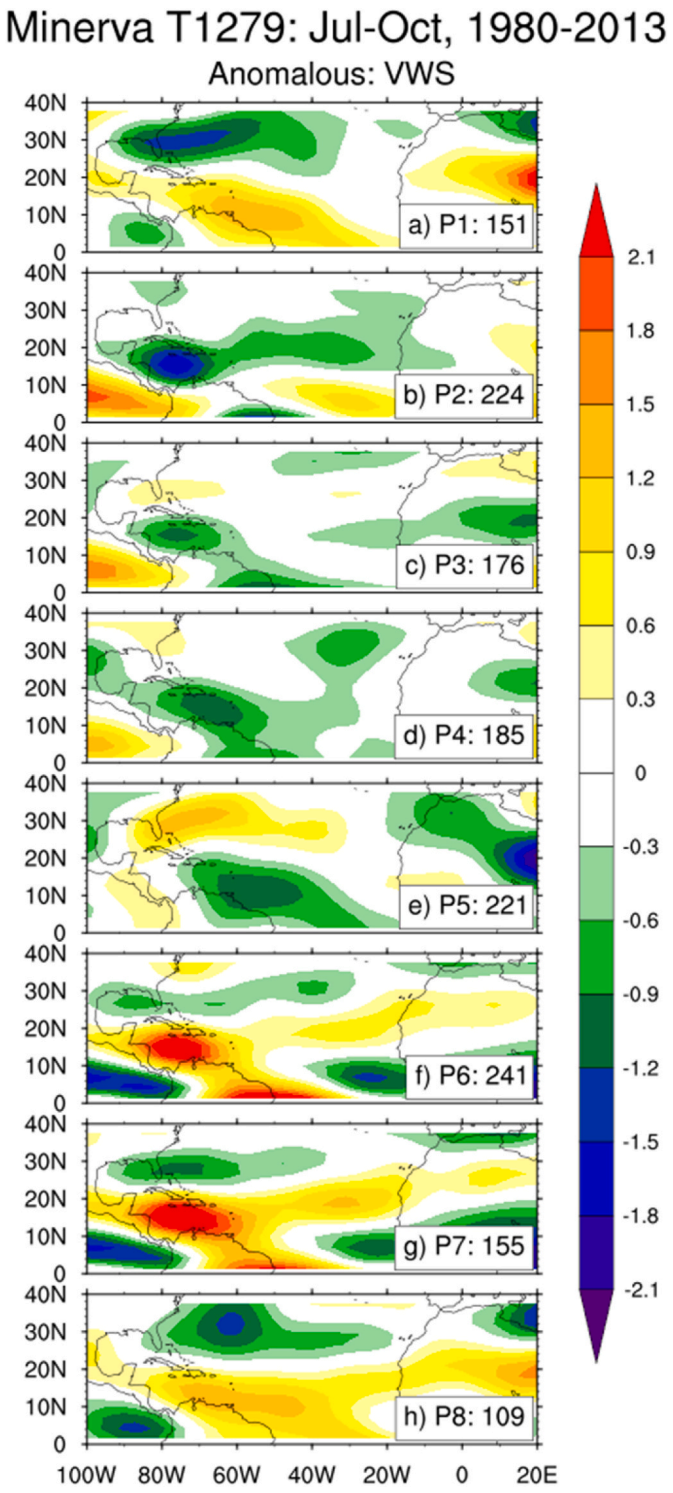

Fig. 6. Minerva T1279 JASO (1980–2013) composites of ensemble-mean anomalous vertical wind shear for each MJO phase (indicated in the caption of each panel after letter "P") using the VPM index. Composites are made by averaging over the set of all days for a particular phase when the MJO amplitudes are greater or equal to one standard deviation. Total number of days is listed in the caption of each panel. Units are ms^{-1}.

captures more of the life cycle of the simulated storms than it is done in operational analyses (see more discussion below).

We next investigate whether the phase of the MJO at different lead times[3] modifies the risk of mid-Atlantic TC landfalls. We first look at the probability of such landfalls conditioned on the phase of the MJO. To do so, the land-falling events at leads ranging from 14 days to the landfall and the daily basin-wide TC counts are binned by each phase of the MJO when the corresponding MJO amplitude is greater or equal to one (standard deviation). The ratios of these values accumulated over the JASO season of 1980–2013, multiplied by 100, are displayed in Fig. 4. Confidence intervals are obtained by randomly assigning, without replacement, an MJO phase value to all simulation records as selected above. Landfall probabilities are then computed for each MJO phase based on this synthetic record. This procedure is repeated 10,000 times and the results are sorted. The computed 10% and 90% confidence intervals are displayed by vertical outlined bars in black in Fig. 4. Fig. 4 could be interpreted to answer the following question: "Given that the MJO is in phase X, how would this affect the probability that the current tropical cyclone will make landfall in the mid-Atlantic in Y days?", where X ranges from 1 to 8 and Y from 14 to 0. Although the absolute probability values are small and do not exceed 0.18% (a reflection of how indeed rare these land-falling events are), what matters is whether and how MJO modulates these probabilities. We find that mid-Atlantic TC landfalls are overall more likely to occur during VPM[4] phases 7, 8 and 1–3 compared to phases 4–6, where phase 4 is the least likely to be associated with such events. At longer lead times (between 14- and 7-day leads), statistically significant peak landfall probabilities are present during phases 1 and 7 with some input from phase 8. At shorter lead times (between 6-day lead and landfall), phase 1 is strongly favored with some contribution from phases 2 and 3. The strongest modulation by the MJO clearly takes place during phase 1 at a wide range of lead times. Fig. 4 also indirectly identifies the phases of MJO that are more favorable for the development and steering of TCs with a higher probability of landfall in the mid-Atlantic. When we also factor in the genesis (not considering landfall probabilities, rather landfall frequencies), landfall modulation by the MJO predominantly takes place during phase 1 with smaller influence from phases 2 and 3 (see Fig. S3 in the Supplemental Information), since TC activity is rather minimal in phases 7 and 8 (Fig. 3).

To substantiate the model results described above, Fig. 5 shows statistics similar to Fig. 4, computed based on observational data for the extended period of 1905–2015. The absolute landfall probability magnitudes are overall much higher reaching 0.8% in some cases. We believe this is likely due to shorter TC tracks in observations compared to model extracted tracks as discussed earlier, which in turn results in lower daily basin-wide TC counts on average. The uncertainty range is also quite large due to very few mid-Atlantic TC landfall occurrences in observational data. Despite these differences, there are a number of similarities between the two sets of results. The observed mid-Atlantic TC landfalls are more likely to occur during phases 7, 8 and 1–3 compared to phases 4–6, as in the model, although it is now phase 6, which is the least likely to be associated with these landfalls. At longer lead times (between 14- and 6-day leads), MJO phase 1 clearly stands out as being linked with the highest statistically significant landfall probabilities. There is a weaker influence from phase 7 and possibly phase 8. These results are in agreement with our findings using historical forecast data in Fig. 4. At shorter lead times, observed MJO modulation of TC landfalls is much weaker and is mostly limited to phase 3 and possibly phases 2 and 8, which is partly at odds with the model results. In addition to the uncertainty due to sampling errors (low landfall count)

[3] We refer here to TC landfall leads, or days before landfall. We use the phrase "lead times" in this sense for the remainder of the paper unless otherwise noted.

[4] In Figs. 4 and 5 below, MJO phases from different indices can be interpreted interchangeably. For example, Fig. 4 would look the same using RMM index.

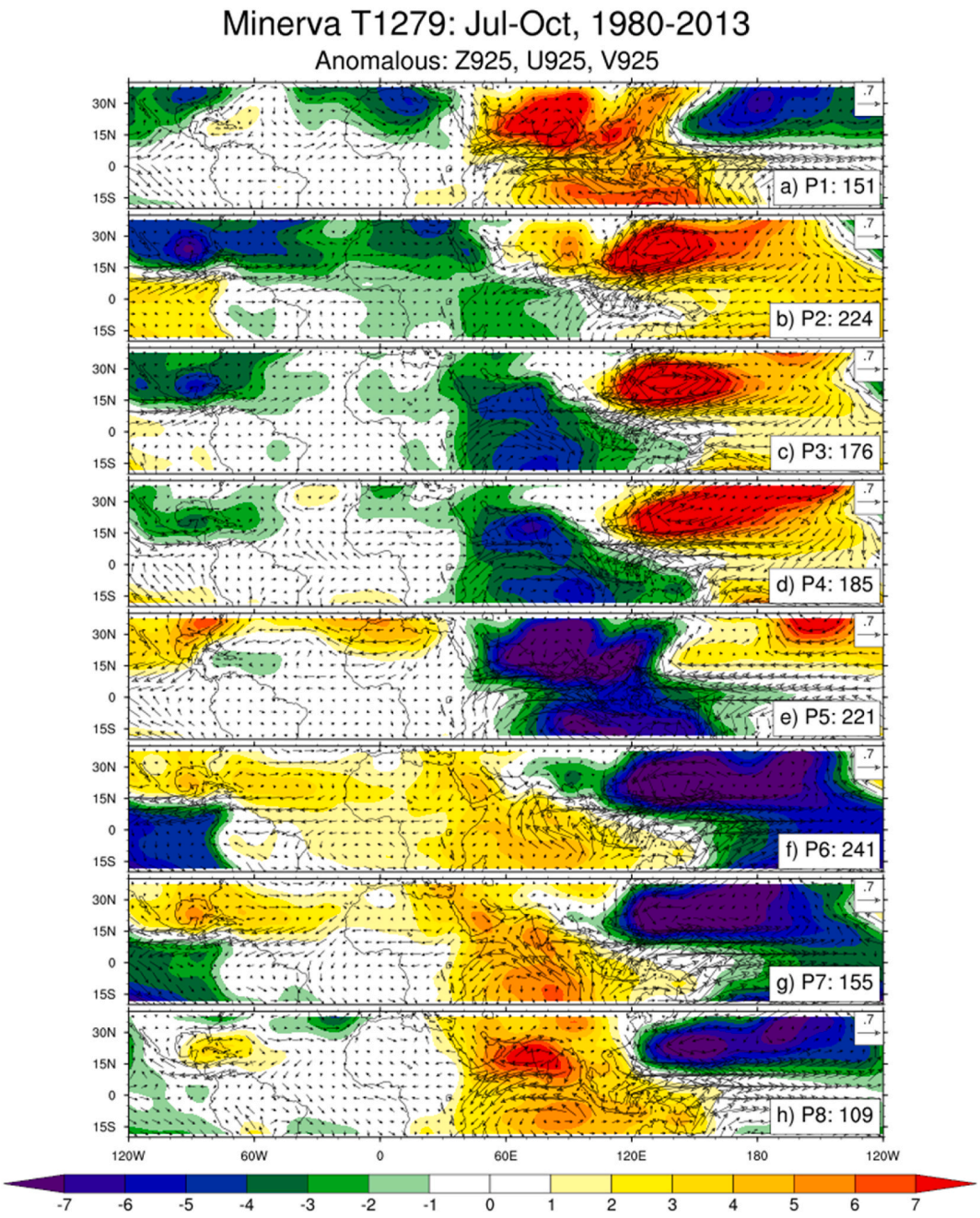

Fig. 7. Minerva T1279 JASO (1980–2013) composites of ensemble-mean anomalous 925-hPa geopotential height (shaded) and 925-hPa wind (vectors) for each MJO phase (indicated in the caption of each panel after letter "P") using the VPM index. Composites are made by averaging over the set of all days for a particular phase when the MJO amplitudes are greater or equal to one standard deviation. Total number of days is listed in the caption of each panel. Units are m. The reference vector is 0.7 ms^{-1}.

and the differences in the TC tracking mentioned above, deviations between the model and observational results could also be due to the different time periods analyzed (see Klotzbach and Oliver, 2015) and perhaps some differences in the MJO phase diagnostics.

4. Discussion and conclusions

This study investigates the MJO modulation of mid-Atlantic TC landfalls using seasonal hindcasts performed with an ensemble prediction system based on the ECMWF model operational in 2012 (Project Minerva) to simulate these rare events. Minerva retrospective forecasts utilized here have high horizontal resolution in their atmospheric component model corresponding approximately to 16-km grid spacing. They have been previously shown to achieve reasonable skill in predicting the North Atlantic basin-wide and regional seasonal TC activity including in the vicinity of the U.S. mid-Atlantic region (Manganello et al., 2016). Minerva forecasts are also skillful in their representation of basic statistical characteristics and climatological features of these land-falling events, which in addition have been found to be predictable on synoptic time scales (Manganello et al., 2019).

Using the VPM index of Ventrice et al. (2013) to diagnose the daily phase and amplitude of the MJO, we find that mid-Atlantic TC landfalls have higher probability of occurrence during certain VPM phases compared to others. Specifically, in the extended range (between 14 and 7 days prior to landfall) phases 1 and 7, and perhaps 8, are mostly favored, a result that is largely supported by observational data. In the

short range, it is mainly phase 1 that has influence, with some contribution from phases 2 and 3. This potential predictability in the longer range is of particular interest, as it has not received much attention. It could stem from the following factors: (1) convectively active MJO phase reaches the Caribbean Sea and the Gulf of Mexico during phases 7 and 8 and extends over the whole tropical North Atlantic in phase 1 (see Figs. 1 and 2); (2) convection associated with the MJO is also enhanced over tropical Africa during phases 8 and 1 although convective anomalies are weaker in the model during phase 8 compared to observations; (3) African convective signals could lead to enhanced AEW activity during phase 1 (Ventrice et al., 2011); (4) reduced VWS establishes east of Florida (one of the genesis centers (see Fig. 2 in Manganello et al. (2019)) during phase 7 and extends to central North Atlantic in phases 8 and 1 (see Fig. 6). The above environmental conditions could favor formation and initial development of the land-falling TCs, and the in-depth analysis of their influences and interactions in relation to the extended-range predictions of mid-Atlantic TC landfalls would be the subject of future work.

Our results are also consistent with a number of previous studies. Klotzbach (2010) has found that the highest levels of the Atlantic TC activity, including the U.S. landfalls, take place during RMM phases 1 and 2 in association with reduced VWS, anomalously high moisture and enhanced low-level cyclonic relative vorticity. In the work of Ventrice et al. (2011), RMM phases 1–3 are the most favorable for the tropical cyclogenesis in the main development region (MDR; 5°-25°N, 60°-15°W) due to similar large-scale environmental changes and enhanced AEW activity over tropical Africa. The latter results have been largely confirmed by Ventrice et al. (2013) using the VPM index. Similarly, Minerva hindcasts show reduced VWS over the western tropical North Atlantic during the VPM phase 1, in the eastern Caribbean, MDR and off the coast of West Africa during phase 2 and, to a lesser extent, phase 3 (Fig. 6). Reduced lower-tropospheric geopotential height and westerly wind anomalies implying enhanced cyclonic vorticity are also present over tropical North Atlantic and western Africa during phases 1–3 (see Fig. 7). An indication of enhanced convection over the Indian Ocean during VPM phases 2 and 3 (Figs. 3 and 7) is also consistent with the analysis of Hurricane Sandy's westward steering flow by Ding et al. (2019). While all these factors point in the right direction, additional work is needed to better understand the intraseasonal forcings and mechanisms responsible for these land-falling events. That is, how remote extratropical teleconnections that modulate the steering flow as suggested by Ding et al. (2019), tropical pathways like AEWs and equatorial Rossby waves (see Ventrice et al., 2011) and local influences by means of large-scale environmental changes, within the envelope of the MJO, impact the genesis, development and tracks of TCs that eventually make landfall over the U.S. mid-Atlantic region.

The clear implication of this study is the potential for extended-range forecasts of the mid-Atlantic TC landfall risk based on the phase of the MJO. The knowledge of the MJO phase can increase the landfall probabilities by up to a factor of three, though the overall magnitudes remain very low. Nonetheless, probabilities in this range are fairly common in probabilistic forecasting of locally extreme precipitation in the medium range (e.g., Herman and Schumacher, 2018). An alternative approach to the one taken in this study would be to use the risk ratio as a forecasting metric. It is defined as a ratio of forecast probabilities to some base probability, e.g., climatological probability. This metric has been used, for instance, in predictions of rare, high-impact weather events, like extreme floods and droughts (van der Wiel et al., 2018; Li et al., 2021). In addition, state-of-the-art ensemble prediction systems display significant skill in MJO forecasting beyond two weeks (e.g., Vitart, 2017). This progress along with recent improvements in the dynamical predictions of the TC genesis risk in the same time range would make such undertaking feasible.

CRediT authorship contribution statement

Julia V. Manganello: Conceptualization, Data curation, Formal analysis, Investigation, Methodology, Validation, Visualization, Writing – original draft. **James L. Kinter:** Funding acquisition, Project administration, Resources, Software, Supervision, Writing – review & editing.

Declaration of competing interest

The authors declare that they have no known competing financial interests or personal relationships that could have appeared to influence the work reported in this paper.

Acknowledgments

Funding of COLA for this study is provided by grants from NSF (AGS-1338427), NOAA (NA14OAR4310160), and NASA (NNX14AM19G). Special thanks to the European Centre for Medium-Range Weather Forecasts, particularly Franco Molteni and Frederic Vitart, for designing, planning, and conducting some of the simulations as part of the Minerva project. A publicly available version of the ECMWF code can be found at https://confluence.ecmwf.int//display/OIFS/OpenIFS+Home. Computing resources on the Yellowstone supercomputer provided by the National Center for Atmospheric Research and the NCAR Command Language scripts available at https://www.ncl.ucar.edu are also gratefully acknowledged.

Appendix A. Supplementary data

Supplementary data to this article can be found online at https://doi.org/10.1016/j.wace.2021.100387.

References

Balmaseda, M.A., Mogensen, K., Weaver, A.T., 2013. Evaluation of the ECMWF ocean reanalysis system ORAS4. Q. J. R. Meteorol. Soc. 139, 1132–1161.

Barrett, B.S., Leslie, L.M., 2009. Links between tropical cyclone activity and Madden-Julian oscillation phase in the north Atlantic and Northeast Pacific basins. Mon. Weather Rev. 137, 727–744. https://doi.org/10.1175/2008MWR2602.1.

Bell, G.D., Halpert, M.S., Schnell, R.C., Higgins, R.W., Lawrimore, J., Kousky, V.E., Tinker, R., Thiaw, W., Chelliah, M., Artusa, A., 2000. Climate assessment for 1999. Bull. Am. Meteorol. Soc. 81, 1328.

Blake, E.S., Kimberlain, T.B., Berg, R.G., Cangialosi, J.P., Beven II, J.L., 2013. Tropical cyclone Report, hurricane Sandy (22–29 October 2012). In: NHC Tech. Rep. AL182012. National Hurricane Center, p. 157. https://www.nhc.noaa.gov/data/tcr/AL182012_Sandy.pdf.

Dailey, P.S., Zuba, G., Ljung, G., Dima, I.M., Guin, J., 2009. On the relationship between the North Atlantic sea surface temperatures and U.S. hurricane landfall risk. J. Appl. Meteor. and Clim 48, 111–129. https://doi.org/10.1175/2008JAMC1871.1.

Dee, D.P., et al., 2011. The ERA-Interim reanalysis: configuration and performance of the data assimilation system. Q. J. R. Meteorol. Soc. 137, 553–597. https://doi.org/10.1002/qj.828.

Ding, L., Li, T., Xiang, B., Peng, M., 2019. On the westward turning of Hurricane Sandy (2012): effect of atmospheric intraseasonal oscillations. J. Clim. 32, 6859–6873. https://doi.org/10.1175/JCLI-D-18-0663.1.

European Centre for Medium-Range Weather Forecasts, 2013. IFS Documentation—CY38r1. ECMWF. https://www.ecmwf.int/en/forecasts/documentation-and-support/changes-ecmwf-model/ifs-documentation. (Accessed 12 September 2018).

Gottschalck, J., Wheeler, M., Weickmann, K., Vitart, F., Savage, N., Lin, H., Hendon, H., Waliser, D., Sperber, K., Prestrelo, C., Nakagawa, M., Flatau, M., Higgins, W., 2010. A framework for assessing operational model MJO forecasts: a project of the CLIVAR Madden – Julian Oscillation Working Group. Bull. Am. Meteorol. Soc. 91, 1247–1258. https://doi.org/10.1175/2010BAMS, 2816.1.

Herman, G.R., Schumacher, R.S., 2018. Money doesn't grow on trees, but forecasts do: forecasting extreme precipitation with random forests. Mon. Weather Rev. 146, 1571–1600. https://doi.org/10.1175/MWR-D-17-0250.1.

Hodges, K.I., 1994. A general method for tracking analysis and its application to meteorological data. Mon. Weather Rev. 122, 2573–2586. https://doi.org/10.1175/1520-0493(1994)122<2573. AGMFTA>2.0.CO;2.

Hodges, K.I., 1995. Feature tracking on the unit sphere. Mon. Weather Rev. 123, 3458–3465. https://doi.org/10.1175/1520-0493(1995)123<3458. FTOTUS>2.0.CO;2.

Hodges, K.I., 1999. Adaptive constraints for feature tracking. Mon. Weather Rev. 127, 1362–1373. https://doi.org/10.1175/1520-0493(1999)127<1362:ACFFT>2.0.CO,2.

Huang, C.S.Y., Nakamura, N., 2016. Local finite-amplitude wave activity as a diagnostic of anomalous weather events. J. Atmos. Sci. 73, 211–229. https://doi.org/10.1175/JAS-D-15-0194.1.

Jiang, X., Xiang, B., Zhao, M., Li, T., Lin, S.-J., Wang, Z., Chen, J.-H., 2018. Intraseasonal tropical cyclone genesis prediction in a global coupled model system. J. Clim. 31, 6209–6227. https://doi.org/10.1175/JCLI-D-17-0454.1.

Klotzbach, P.J., 2010. On the Madden-Julian oscillation – Atlantic hurricane relationship. J. Clim. 23, 282–293. https://doi.org/10.1175/2009JCLI2978.1.

Knapp, K.R., Kruk, M.C., Levinson, D.H., Diamond, H.J., Neumann, C.J., 2010. The international best track Archive for climate stewardship (IBTrACS). Bull. Am. Meteorol. Soc. 91, 363–376.

Klotzbach, P.J., Oliver, E.C., 2015. Modulation of Atlantic basin tropical cyclone activity by the Madden-Julian Oscillation (MJO) from 1905 to 2011. J. Clim. 28, 204–217. https://doi.org/10.1175/JCLI-D-14-00509.1.

Lee, C.-Y., Camargo, S.J., Vitart, F., Sobel, A.H., Tippett, M.K., 2018. Sub-seasonal tropical cyclone genesis prediction and MJO in the S2S dataset. Weather Forecast. 33, 967–988. https://doi.org/10.1175/WAF-D-17-0165.1.

Lee, C.-Y., Camargo, S.J., Vitart, F., Sobel, A.H., Camp, J., Wang, S., Tippett, M.K., Yang, Q., 2020. Subseasonal predictions of tropical cyclone occurrence and ACE in the S2S dataset. Weather Forecast. 35, 921–938. https://doi.org/10.1175/WAF-D-19-0217.1.

Li, T., 2014. Recent advance in understanding the dynamics of the Madden-Julian oscillation. J. Meteor. Res. 28 (1), 1–33. https://doi.org/10.1007/s13351-014-3087-6.

Li, W., Pan, R., Jiang, Z., Chen, Y., Li, L., Luo, J.-J., Zhai, P., Shen, Y., Yu, J., 2021. Future changes in the frequency of extreme droughts over China based on two large ensemble simulations. J. Clim. 34, 6023–6035. https://doi.org/10.1175/JCLI-D-20-0656.1.

Madden, R.A., Julian, P.R., 1994. Observations of the 40-50-day tropical oscillation – a review. Mon. Weather Rev. 122, 814–837.

Madec, G., 2008. NEMO ocean engine. Note du Pole de modélisation, Institut Pierre-Simon Laplace (IPSL). Tech. Rep. 27, 396. https://www.nemo-ocean.eu/wp-content/uploads/NEMO_book.pdf.

Manganello, J.V., et al., 2016. Seasonal forecasts of tropical cyclone activity in a high-atmospheric-resolution coupled prediction system. J. Clim. 29, 1179–1200. https://doi.org/10.1175/JCLI-D-15-0531.1.

Manganello, J.V., Cash, B.A., Swenson, E.T., Kinter III, J.L., 2019. Assessment of climatology and predictability of mid-Atlantic tropical cyclone landfalls in a high-atmospheric-resolution seasonal prediction system. Mon. Weather Rev. 147, 2901–2917. https://doi.org/10.1175/MWR-D-19-0107.1.

Mo, K.C., 2000. The association between intraseasonal oscillations and tropical storms in the Atlantic basin. Mon. Weather Rev. 128, 4097–4107.

Nhc, 2018. Costliest U.S. Tropical Cyclones Tables Updated. National Hurricane Center, p. 3. https://www.nhc.noaa.gov/news/UpdatedCostliest.pdf. (Accessed 29 May 2018).

Oliver, E.C.J., Thompson, K.R., 2012. A reconstruction of Madden-Julian Oscillation variability from 1905 to 2008. J. Clim. 25, 1996–2019. https://doi.org/10.1175/JCLI-D-11-00154.1.

Shen, B.-W., DeMaria, M., Li, J.-L.F., Cheung, S., 2013. Genesis of Hurricane Sandy (2012) simulated with a global mesoscale model. Geophys. Res. Lett. 40, 4944–4950. https://doi.org/10.1002/grl.50934.

van der Wiel, K., Kapnick, S.B., Vecchi, G.A., Smith, J.A., Milly, P.C.D., Jia, L., 2018. 100-Year lower Mississippi floods in a global model: characteristics and future changes. J. Hydrometeorol. 19, 1547–1563. https://doi.org/10.1175/JHM-D-18-0018.1.

Ventrice, M.J., Thorncroft, C.D., Roundy, P.E., 2011. The Madden-Julian Oscillation's influence on African easterly waves and downstream tropical cyclogenesis. Mon. Weather Rev. 139, 2704–2722. https://doi.org/10.1175/MWR-D-10-05028.1.

Ventrice, M.J., Wheeler, M.C., Hendon, H.H., Schreck III, C.J., Thorncroft, C.D., Kiladis, G.N., 2013. A modified multivariate Madden-Julian Oscillation index using velocity potential. Mon. Weather Rev. 141, 4197–4210. https://doi.org/10.1175/MWR-D-12-00327.1.

Vitart, F., 2009. Impact of the Madden Julian Oscillation on tropical storms and risk of landfall in the ECMWF forecast system. Geophys. Res. Lett. 36, L15802. https://doi.org/10.1029/2009GL039089.

Vitart, F., 2017. Madden-Julian Oscillation prediction and teleconnections in the S2S database. Q. J. R. Meteorol. Soc. 143, 2210–2220. https://doi.org/10.1002/qj.3079.

Wheeler, M.C., Hendon, H.H., 2004. An all-season real-time multivariate MJO index: development of an index for monitoring and prediction. Mon. Weather Rev. 132, 1917–1932.

Xiang, B., et al., 2015. Beyond weather time-scale prediction for hurricane Sandy and super typhoon haiyan in a global climate model. Mon. Weather Rev. 143, 524–535. https://doi.org/10.1175/MWR-D-14-00227.1.